Exploration of the extracellular matrix of the red alga Chondrus crispus reveals unprecedented insights into carrageenan structures

David Ropartz, Adrien Lissarrague, Murielle Jam, Diane Jouanneau, Bastien Annic, Sophie Le Gall, Mathieu Fanuel, Stacy Krueger-Hadfield, Myriam Valéro, Mirjam Czjzek, et al.

▶ **To cite this version:**

David Ropartz, Adrien Lissarrague, Murielle Jam, Diane Jouanneau, Bastien Annic, et al.. Exploration of the extracellular matrix of the red alga Chondrus crispus reveals unprecedented insights into carrageenan structures. Carbohydrate Polymers, 2025, 348, pp.122737. ⟨10.1016/j.carbpol.2024.122737⟩. ⟨hal-04734206⟩

HAL Id: hal-04734206

https://hal.science/hal-04734206v1

Submitted on 13 Oct 2024

HAL is a multi-disciplinary open access archive for the deposit and dissemination of scientific research documents, whether they are published or not. The documents may come from teaching and research institutions in France or abroad, or from public or private research centers.

L'archive ouverte pluridisciplinaire **HAL**, est destinée au dépôt et à la diffusion de documents scientifiques de niveau recherche, publiés ou non, émanant des établissements d'enseignement et de recherche français ou étrangers, des laboratoires publics ou privés.

Distributed under a Creative Commons CC BY 4.0 - Attribution - International License

Carbohydrate Polymers 348 (2025) 122737

Contents lists available at ScienceDirect

Carbohydrate Polymers

journal homepage: www.elsevier.com/locate/carbpol

Exploration of the extracellular matrix of the red alga *Chondrus crispus* reveals unprecedented insights into carrageenan structures

David Ropartz [a,b], Adrien Lissarrague [a,b], Murielle Jam [c], Diane Jouanneau [c], Sophie Le Gall [a,b], Bastien Annic [a,b], Mathieu Fanuel [a,b], Stacy A. Krueger-Hadfield [d], Myriam Valéro [e], Mirjam Czjzek [c], Hélène Rogniaux [a,b,*], Cécile Hervé [c]

[a] *INRAE, URBIA, F-44316 Nantes, France*
[b] *INRAE, PROBE Research Infrastructure, BIBS Facility, F-44316 Nantes, France*
[c] *Integrative Biology of Marine Models (LBI2M), UMR8227, Station Biologique de Roscoff (SBR), CNRS, Sorbonne Université, 29680 Roscoff, France*
[d] *Virginia Institute of Marine Science Eastern Shore Laboratory, Wachapreague, VA 23480, USA*
[e] *CNRS, Sorbonne Université, Pontificia Universidad Católica de Chile, Universidad Austral de Chile, IRL 3614, Evolutionary Biology and Ecology of Algae, Station Biologique de Roscoff, Roscoff, France*

ARTICLE INFO

Keywords:
Carrageenans
Chondrus crispus
Life cycle phase
Glycosyl hydrolase
Mass spectrometry
Structural diversity

ABSTRACT

Carrageenans are major gel forming polysaccharides in the extracellular matrix of the red macroalga *Chondrus crispus*. These galactans are made of linear chains of repetitive disaccharide motifs based on D-galactose residues alternately linked by β-1,4 and α-1,3 glycosidic bonds. A definite number of disaccharide motifs are known, based on their regular sulfations and the presence of a 3,6-anhydro bridge. While these motifs are variable as a function of species, life cycle phases, or seasons, our understanding of the in vivo regulation of carrageenan fine structures is still limited. Characterized hydrolytic enzymes (κ-, ι- and λ-carrageenases) are powerful tools for identifying glycan structures in extracted ECMs. Their use, combined to chromatography and high-resolution mass spectrometry, allowed us to refine our understanding of carrageenan variability in the phases of *C. crispus*. We provide the first demonstration that κ/ι carrabiose motifs are not limited to gametophytes, but are also present in tetrasporophytes, together with over- and under-sulfated λ-motifs. Our findings highlight a more complex carrageenan composition than previously described in this model system. These results are further discussed in the light of recent transcriptomic data and suggest that the historical hypotheses on the biosynthetic pathway of carrageenans in red algae may need revision.

Hypothesis: Combined characterized hydrolytic enzymes to chromatography and high-resolution mass spectrometry can refine our understanding of carrageenan variability in the phases of *C. crispus*.

1. Introduction

Chondrus crispus is a red macroalga in the family *Gigartinaceae*. The availability of its genome (Collen et al., 2013) makes it an ideal research model for transcriptomic analyses (Lipinska, Collen, Krueger-Hadfield, Mora, & Ficko-Blean, 2020) and gene identification This red alga possesses an extracellular matrix (ECM)—or cell wall—that is crucial for ensuring the structural integrity of its thallus and biological functions such as cell-to-cell communication, development and defence responses (Bouarab, Potin, Correa, & Kloareg, 1999; Chevenier, Jouanneau, & Ficko-Blean, 2023; Collen et al., 2014; Kloareg, Badis, Cock, & Michel, 2021). The ECM consists of a complex supramolecular network mainly composed of polyanionic polysaccharides, known as carrageenans. *Chondrus crispus* is thus important not only for coastal ecology, but also for economy, as an important producer of carrageenans used in several industries (Ahmadi, Moghadamtousi, Abubakar, & Zandi, 2015; Cheong, Qiu, Du, Liu, & Khan, 2018; Dong, Wei, & Xue, 2021; Pacheco-Quito, Ruiz-Caro, & Veiga, 2020; Rupert, Rodrigues, Thien, & Yong, 2022; Zia et al., 2017).

Carrageenans are linear chains of a repetitive disaccharide pattern, composed of D-galactose units alternately linked by β-1,4 and α-1,3 linkages. Most often, the β-linked dimer consists of D-galactose-4-sulfate and 3,6-anhydro-D-galactose, a bicyclic sugar unique to red macroalgae (Collen et al., 2013) (Table S1). However, these repeating subunits can

* Corresponding author at: INRAE, PROBE Research Infrastructure, BIBS Facility, F-44316 Nantes, France.
E-mail address: Helene.rogniaux@inrae.fr (H. Rogniaux).

https://doi.org/10.1016/j.carbpol.2024.122737
Received 22 March 2024; Received in revised form 6 September 2024; Accepted 9 September 2024
Available online 20 September 2024
0144-8617/© 2024 The Authors. Published by Elsevier Ltd. This is an open access article under the CC BY license (http://creativecommons.org/licenses/by/4.0/).

vary widely (additional sulfate functions, absence of anhydro bridges, etc.). Carrageenans naturally occur as heteropolymers, with an alternation of chemically diverse moieties that give them a specific three-dimensional structural organization and specific resulting properties. The occurrence of 3,6-anhydro-bridges, for instance, promotes the formation of helices in the carrageenan chain, which then forms gel-networks.

In *C. crispus*, composition of ECM carrageenans vary significantly according to the life cycle phase of the alga. *Chondrus crispus* has a complex haploid-diploid life cycle alternating between male and female gametophytes (haploid, n) and tetrasporophytes (diploid, 2n). Carrageenan in *C. crispus* gametophytes (female or male) are described as being mainly composed by kappa (κ) (1→3) linked β-D-galactose-4-sulfate-(1→4)-3,6-anhydro-α-D-galactose, and iota (ι) (1→3) linked β-D-galactose-4-sulfate-(1→4)-3,6-anhydro-α-D-galactose-2-sulfate carrabiose units (~70 and 20 %, respectively) (Collen et al., 2014), and their biological precursors, named the μ (mu, (1→3) linked β-D-galactose-4-sulfate-(1→4)-α-D-galactose-6-sulfate) and ν (nu, (1→3) linked β-D-galactose-4-sulfate-(1→4)-α-D-galactose-2,6-disulfate) carrabiose units (~8 and 2 %, respectively) (Table S1). In contrast, the ECM of the tetrasporophyte is described as being composed almost exclusively of lambda-carrageenans (λ) based on (1→3) linked β-D-galactose-2-sulfate-(1→4)-D-galactose-2,6-disulfate carrabiose units (Table S1) (García Tasende, Cid, & Fraga, 2012; Guibet, 2007; McCandless, Craigie, & Walter, 1973). The difference in ECM composition between tetrasporophytes and gametophytes confer these two phases with different chemical and rheological properties (Cheong, Qiu, Du, Liu, & Khan, 2018; Kloareg, Badis, Cock, & Michel, 2021). Notably, it is usually believed that no compositional difference can be found in the ECMs of male and female gametophytes, although this has never been shown for definite, essentially due to the isomorphic appearance of the thalli and the supposed rarity of male plants in the field (Krueger-Hadfield, Roze, Correa, Destombe, & Valero, 2015; Krueger-Hadfield, Roze, Mauger, & Valero, 2013; Lipinska, Collen, Krueger-Hadfield, Mora, & Ficko-Blean, 2020).

The variation of carrageenan structures among *C. crispus* phases would imply a very tight control of expression of the ECM-genes. The putative carrageenan biosynthetic pathway was first proposed in 1979 (Craigie & Wong, 1979) and later updated (Ficko-Blean, Hervé, & Michel, 2015). Most steps have been suggested based on the chemical diversity of the constitutive carrabiose units. They would call up a series of galactosyltransferases, carbohydrate-sulfotransferases and galactose-sulfurylases; the latter catalysing the formation of the 3,6-anhydro-D-galactose molecule through the removal of a sulfate group, as found for instance in the κ and ι carrabiose units. Investigations of transcriptomic data on the three phases of the referenced *C. crispus* strain (Lipinska, Collen, Krueger-Hadfield, Mora, & Ficko-Blean, 2020) surprisingly indicate that these predicted ECM-genes were only partially differentially regulated among the phases. In particular, 10 of the 16 galactose-sulfurylase genes were upregulated in *C. crispus* tetrasporophytes compared to gametophytes, a rather counterintuitive result since the tetrasporophytes are known to contain mainly λ-carrageenan, and therefore devoid of 3,6-anhydro rings (García Tasende, Cid, & Fraga, 2012; Guibet, 2007; McCandless, Craigie, & Walter, 1973). Beyond the dominant galactan structures found in a specific thallus, it is thus very likely that other carrageenan moieties are expressed but still uncharacterized.

In addition, beyond their chemical details, the way carrageenans are interconnected at the macromolecular scale to shape a cohesive ECM network is not well understood. In *C. crispus*, the phases are almost mechanically equivalent (Carrington, Grace, & Chopin, 2001), yet their carrageenan types differ with a strong impact on their rheological properties. Since pure λ-carrageenans do not feature 3,6-anhydro-bridges as κ- and ι-carrageenans, they do not form physical gels, but only highly viscous solutions because their conformation makes it impossible to form helices. This questions how cell wall polymers in the tetrasporophytes, with a λ-carrageenan dominance, can contribute to the mechanical resistance of the wall. Minor components and/or polymer interactions, both yet to be described, may have possible contribution in this mechanics. In land plants, amorphous polysaccharides of the cell wall form bridges with crystalline polysaccharides (mostly cellulose fibrils), thereby strengthening the mechanical resistance of the wall (Peaucelle, Braybrook, & Hoefte, 2012). Such architecture could occur in red algae as well, but has yet to be established experimentally. Furthermore, in red algae, crystalline polysaccharides represent a small portion of the ECM (1–8 % of the dry weight). Cellulose fibrils are the most common crystalline polymer but the presence of cellulose has never been clearly established in the ECM of *C. crispus*, despite two cellulose synthases found in the genome (Collen et al., 2013). Additional hemicellulosic components are not known to occur in *C. crispus* or more generally in the Gigartinales order.

Knowing how components interact and are organized in the ECM is essential for understanding the biological or functional properties of red algae. A first step towards this goal is to describe the chemical diversity of the underlying polysaccharide structures, which still represent a true analytical challenge. First, carrageenans are entangled within the context of a complex ECM and are not easily extractible from this network. Additionally, the structural diversity of carrageenans is based on a variety of building blocks that involve numerous isomeric units. This is combined with a high degree of sulfation which is a labile modification that can easily be lost during chemical analysis. Finally, most current methods for compositional analysis lose the connectivity of the blocks within the polymeric chain, whereas this distribution is decisive for the understanding of the structure and of the physico-chemical properties of carrageenans and their role in the ECM. In this context, a greater progress on their structural characterization were made using specific and characterized enzymes from marine bacteria (i.e. κ-carrageenases (Collen et al., 2009; Guibet et al., 2008), ι-carrageenases (Guibet et al., 2008; Prechoux & Helbert, 2014), and λ-carrageenases (Guibet et al., 2007; Guibet, Kervarec, Genicot, Chevolot, & Helbert, 2006)) in combination with NMR (Jouanneau, Boulenguer, Mazoyer, & Helbert, 2010; Vilen, Lundqvist, Jouanneau, Helbert, & Sandstrom, 2010) and mass spectrometry methods (Anastyuk et al., 2011; Yermak et al., 2021).

Our aim was to contribute to the chemical understanding of carrageenans and their structure-function relationship, by establishing the most complete picture of the chemical structures of carrageenans present in the life cycle phases of *C. crispus*, including some minor structures that may contribute to the mechanical properties of the ECM. The present work explored in details the ECM-carrageenans of tetrasporophytes as well as of male and female gametophytes from *C. crispus* thalli isolated from natural rocky shore populations. We used a combination of morphology, molecular biology, biochemistry, and analytical and structural chemistry. In particular, we produced a global chemical composition of the ECM; we then used specific carrageenases to produce complex mixtures of oligosaccharides (OS) that were further characterized by high pressure size exclusion chromatography refractive index (HPSEC-RI) and ultra-high performance liquid chromatography coupled with high resolution mass spectrometry (UHPLC-HR-MS). The ultimate goal was to determine the structures released to identify whether non-ideal patterns were present in the ECMs. These results also open towards some indirect evidence about the enzymes specificities, in particular about which hybrid character of the substrate they may tolerate.

2. Methods

2.1. Chemicals and reagents

Hexylamine, acetic acid, lithium nitrate, sodium azide, Tris, silver nitrate, acetate and resorcinol were purchased from Sigma-Aldrich Co. (Saint Quentin Fallavier, France). Water was of ultrapure quality,

obtained from a Milli-Q apparatus (Millipore). HPLC-grade acetonitrile (ACN), HCl, ethanol, chloroform, methanol and acetone were purchased from Carlo-Erba Reagents (Val de Reuil, France).

2.2. Biological samples

Chondrus crispus fronds were collected in the North coast of Brittany in France at the Pointe de Bloscon of Roscoff (48.726° N–3.969°W) in February 2010 and described in detail in Krueger-Hadfield, Roze, Mauger, and Valero (2013). Thalli were collected every 25 cm in a 5 m × 5 m grid at ~2 m above mean low water (MLW) in the 'low shore population' described in Krueger-Hadfield, Roze, Mauger, and Valero (2013). We determined whether a thallus was a tetrasporophyte, female gametophyte, or male gametophyte based on the presence of reproductive structures (tetrasporangial sori, cystocarps, or spermatangial sori, respectively) following the procedure previously described (Krueger-Hadfield, Roze, Mauger, & Valero, 2013; Lipinska, Collen, Krueger-Hadfield, Mora, & Ficko-Blean, 2020). We carefully excised the cystocarps from the female prior to preservation in silica gel in 2010 when thalli were freshly collected from the field (see Krueger-Hadfield, Roze, Correa, Destombe, & Valero, 2015). Each thallus was preserved in silica gel and stored in an air tight container. We selected three pools of twelve thalli each from these collections (Table S2): female and male gametophytes (Gf and Gm, respectively), and tetrasporophytes (Ts).

Additional pools were constituted for Gf High quadra (HQ) and Ts HQ from thalli collected in a high shore grid at ~3.6 m above MLW to evaluate variations in ECM composition within a shore (Lazo, Greenwell, & Mclachlan, 1989).

2.3. Resorcinol test

The resorcinol test was performed to provide colorimetric differentiation of tetrasporophytes relative to gametophytes (Yaphe & Arsenault, 1965). A 13.6 mM stock resorcinol solution was prepared by diluting 30 mg of powdered resorcinol in 20 mL of distilled water (stored in the dark). The acetal stock solution was made by adding 8 μL of acetal (1,1-diethoxyethane) to 1992 μL water. The reactive resorcinol-acetal solution was made right before use, and 25 mL of concentrated HCl (37 %, commercial) was added to 2.25 mL of the stock resorcinol solution followed by addition of 250 μL of acetal stock solution. Small fragments silica-preserved thalli, approximately 1 mm × 1 mm, were placed in 1.5 mL Eppendorf tubes then 250 μL of the resorcinol-acetal reagent solution was added following previous work (Krueger-Hadfield, Roze, Mauger, & Valero, 2013). The tubes were incubated for 10 min at 80 °C and then cooled on ice for 2 min, followed by a qualitative colorimetric evaluation of the staining. Gametophytes, which carrageenans contain significant amounts of 3,6-anhydro-galactose, result in positive tests and turn the solution a reddish color, while tetrasporophytes result in a negative test (Fig. S2).

2.4. Microsatellite analyses

These analyses are described in detail in Krueger-Hadfield, Roze, Mauger, and Valero (2013), but we describe them briefly here. Total genomic DNA was extracted using Macherey-Nagel Plant DNA kit, following manufacturer's instructions. We used the microsatellite loci Chc_23 (fluorescent label PET), Chc_24 (fluorescent label VIC), Chc_31 (fluorescent label NED), Chc_40 (fluorescent label 6-FAM), Chc_02 (fluorescent label VIC), Chc_03 (fluorescent label 6-FAM), Chc_04 (fluorescent label PET)), and Chc_35 (fluorescent label NED) (Krueger-Hadfield, Roze, Mauger, & Valero, 2013). Multiplex PCRs were performed, amplifying several loci simultaneously using a PT-200 thermocycler (MJ Research, Waltham, MA, USA): M1 was composed of loci Chc_23, Chc_24, Chc_31, Chc_40 and M2 was composed of loci Chc_02, Chc_03, Chc_04. Two μL of each PCR product, diluted to 1:10, was added to 10 μL of loading buffer containing 0.3 μL of size standard (GeneScan — 600 Liz, Applied Biosystems, Foster City, CA, USA) plus 9.7 μL of Hi-Di formamide (Applied Biosystems, Foster City, CA, USA). The loading mix was denatured at 92 °C for 3 min and run in an ABI 3130 xl capillary sequencer (Applied Biosystems, Foster City, CA, USA) equipped with 50 cm capillaries. Genotypes were scored manually using GENEMAPPER ver. 4 (Applied Biosystems, Foster City, CA, USA) following (Krueger-Hadfield, Roze, Mauger, & Valero, 2013). Multilocus genotypes were then compared to the results from the resorcinol tests to verify all gametophytes displayed one allele per locus and tetrasporophytes displayed one or two alleles per locus (i.e., homozygotes or heterozygotes; see more discussion in Krueger-Hadfield, Roze, Mauger, & Valero, 2013; Krueger-Hadfield, Collen, Daguin-Thiebaut, & Valero, 2011).

2.5. ECM extraction

The entire protocol in schematized in Fig. S1. The samples were dried, finely ground and exhaustively washed sequentially in 70 % ethanol, 80 % ethanol, 96 % ethanol, chloroform:methanol (1:1, v/v) and acetone. The resulting alcohol insoluble residues (AIR) were air-dried overnight. Hundred mg of each AIR were dissolved into 10 mL of milli-Q water and carrageenans were hot-extracted (80 °C, 2 h). After centrifugation, pellets (residues, R) were freeze-dried and stored at room temperature in a dry atmosphere. The S supernatant fractions, containing carrageenans, were dialyzed (6–8 kDa MWCO Spectra/Por®) against distilled water to remove excess of salt and non-polymeric materials. A supernatant (S) and a residue (R) fraction were obtained for each pool.

2.6. Production of the carrageenan degrading enzymes

Three specific enzymes were produced to perform enzymatic degradation of the samples. A recombinant *Pseudoalteromonas carrageenovora* κ-carrageenase (GH16) was over-expressed in *Escherichia coli* BL21(DE3) and purified by affinity chromatography (referred to as the kappase) (Michel et al., 1999). A recombinant *Zobellia galactanivorans* ι-carrageenase (GH82) was over-expressed in *E. coli* and purified by affinity chromatography (referred to as the iotase) (Sokolova et al., 2024). A wild type *P. carrageenovora* λ-carrageenase (GH150) was produced as previously described (referred to as the lambdase) (Guibet et al., 2007). The enzymes were qualitatively and quantitatively assessed on a SDS-PAGE as shown in Fig. S5.

The hydrolysis conditions for each enzyme were optimized on purified polysaccharides from: i) *Kappaphycus alvareizii* (CP Kelco, described as containing pure κ-carrageenans), ii) *Eucheuma denticulatum* (Danisco, described as containing pure ι-carrageenans), and iii) *Gigartina skottsbergii* (Danisco, described as containing pure λ-carrageenans). Optimal concentrations and temperatures were established as follows: 10 μg/mL at 37 °C for the kappase; 5 μg/mL at 32 °C for the iotase; 0.1 μg/mL at room temperature for the lambdase. The reaction products were analysed by carbohydrate-polyacrylamide gel electrophoresis (C-PAGE), according to the procedure described in Zablackis and Perez (1990) (Fig. S6). Hydrolysis was stopped at different times by boiling the samples.

2.7. Enzymatic hydrolysis of the samples

The supernatant obtained after ECM extraction was digested as shown in Fig. S1 using the optimal hydrolysis conditions defined for each enzyme (see above) and a substrate (carrageenan) concentration of 0.1 %. The supernatants obtained for the Gf and the Gm were digested by the kappase, the iotase and the combination of both enzymes, for one and 5 days (1-D and 5-D). A control with boiled enzymes (called 0-D) was systematically produced. The supernatants obtained for the Ts samples were digested by the lambdase, the combination of lambdase and iotase and of lambdase and kappase. When combined, the enzymes were used at their optimum concentration (10 μg/mL for kappase, 5 μg/

mL for iotase and 0.1 μg/mL for the lambdase) and at the lower optimum temperature of the two enzymes (e.g. 32 °C in case of a mixture of kappase and iotase).

2.8. ECMs monosaccharide composition

Identification and quantification of ECMs neutral sugars were performed by gas-liquid chromatography (GC) after acid degradation. For GC analysis after acidic degradation, each sample (5 mg of AIR, S and R fractions, in triplicate) were hydrolyzed with 2 M trifluoroacetic acid, converted to their alditol acetates and chromatographed on a TG-225 GC Column (30 × 0.32 mm ID) using TRACE™ Ultra Gas Chromatograph (Thermo Scientific™; temperature 205 °C, carrier gas H_2). Standard sugars solution and inositol as internal standard were used for calibration. The amount of 3,6-anhydrogalactose was measured by colorimetric assay with resorcinol reagent as described in Yaphe and Arsenault (1965). Briefly, 2.5 mL of resorcinol reagent (100 mL of HCl 37 %, 9 mL of 1.36 mM resorcinol in H2O, 1 mL of 2.77 mM acetal) was added to 0.5 mL of polysaccharide sample solution in a glass tube. The tubes were placed on ice for 10 min, then 4 min at ambient temperature and subsequently incubated at 80 °C for 10 min. Reactions were cooled on ice for 5 min and the absorbance at 555 nm was read within 15 min. Standard curve was made with fructose (0 to 0.15 mM) and a correction factor of 0.92 for 3,6-anhydrogalactose was applied.

2.9. Molecular mass distribution by HPSEC-RI analysis

The size range of the polymers and their hydrolysis products was assessed by High-performance size-exclusion coupled to refractive index detection (HPSEC-RI). The chromatographic system consisted of a Dionex Ultimate 3000 pump and autosampler, coupled to a refractometer (Optilab rEX™, Wyatt Technology, Inc.) Three columns connected in series were used for separation: Shodex SB-805-, -804 and -803-HQ (8 × 300 mm each), with a separation domain comprised between 10^5 and 4.10^6 g/mol. A 0.1 M lithium nitrate solution containing 0.03 % of sodium azide, filtered on a 0.22 μm Durapore membrane (PES, Millipore) was used as eluent. The elution was performed at 0.5 mL/min and at room temperature (21 °C ± 2 °C).

The samples were prepared with an approximate concentration of 2 mg/mL in milli-Q water. They were then filtered through a 0.45 μm syringe filter before injection (100 μL) and analysis. Data were processed with the software Astra™ (6.1.2.84 version) (Lazo, Greenwell, & Mclachlan, 1989).

2.10. Structural determination of the released oligosaccharides by LC-HR-MS analysis

Chromatographic separation of oligosaccharides produced with the different enzymes and combination of enzymes, and for different times (0-D, 1-D and 5-D) was run on an Ultra High Performance Liquid Chromatography system (UHPLC, Acquity H-Class® Waters, Manchester, UK), mounted with a hypersyl Gold column (1 mm × 100 mm, 1.9 μm) (Thermo scientific, Waltham, Massachusetts, USA). Column was heated at 45 °C and the flow rate was of 0.175 μL/min. A ternary gradient was performed (A: pure water; B: pure acetonitrile; C: 20 mM hexylammonium dissolved in water, and pH value adjusted to 6 with acetic acid) from 16.6 % to 35.0 % of solvent B in 10 min, then up to 63.4 % at 20 min, then maintain at 73.4 % from 20 min to 24.5 min, and then maintain at 16.6 % from 24.5 min to 29.5 min. Solvent C was kept constant at 25 %.

The UHPLC system was coupled with a SELECT SERIES Cyclic IMS instrument (Waters, Wilmslow, UK) (Giles et al., 2019). The experiments were performed in negative electrospray ionization mode on the *m/z* range 300–2000. The Time-of-flight analyser was operated in the V-mode. The source parameters were the following: Capillary voltage 2.5 kV; Cone voltage: 40 V; Source temperature: 100 °C; Desolvation temperature: 280 °C; Desolvation gas: 500 L/h; and Nebulization gas: 5.5 bar.

Data were recorded with the Quartz software (Waters embedded software, release 5) and processed using MzMine software (Pluskal, Castillo, Villar-Briones, & Oresic, 2010). For peak picking, an intensity threshold of 5e2 was used. Species were picked when they had at least one isotope in their pattern. For the quantification, the peak area of each isotope was considered. All the samples were analysed in triplicate.

3. Results

The global strategy followed in the present study is schematized in Fig. S1. Briefly, this strategy involved three steps: the constitution of homogenous pools from morphologically and genetically characterized thalli (step A); the global chemical analysis of the ECM of *C. crispus* samples, including the compositional analysis before and after water extraction of ECM compounds (step B); the enzymatic digestion of the water soluble ECM compounds, both with single enzymes or with combination of enzymes, followed by the structural analysis of the released products by HPSEC-RI and UHPLC-HR-MS (step C). Each of the A, B and C steps are detailed below.

3.1. Identification of life cycle phase and constitution of the pools

The *C. crispus* thalli used in this study were sampled from the intertidal zone. A morphological determination of ploidy and sex was first carried out in the field, based on the presence of reproductive structures and iridescence unique to the gametophytes. To further support the ploidy assessment, we performed the resorcinol test accompanied by microsatellite genotyping that can distinguish gametophytic from tetrasporophytic thalli (Krueger-Hadfield, Roze, Correa, Destombe, & Valero, 2015; Krueger-Hadfield, Roze, Mauger, & Valero, 2013). The colorimetric resorcinol assay was positive for the male (Gm) and female gametophytes (Gf), and negative for the tetrasporophytes (Ts), which supported the initial morphological assessment of phase made in the field (Table S2, Fig. S2). Microsatellite multilocus genotyping also confirmed ploidy, though none of the microsatellites are sex-specific or have sex-specific alleles. All gametophytes exhibited a single allele per locus, whereas the tetrasporophytes had two alleles at five of the six loci used to genotype the thalli (Table S3). Following the assessment of life cycle phase, *C. crispus* thalli were pooled into three homogeneous pools of 12 individuals, denoted Gf, Gm and Ts pools (Table S3).

3.2. Chemical composition of the ECM

The ground algal material from each of the homogenous pools of *C. crispus* individuals was subjected to a sequential solvent extraction leading to a so-called “alcohol insoluble residue” (AIR) enriched in ECM components. The AIR was then air-dried and subjected to extraction in water. Water-extraction resulted in a supernatant (S) and a residue (R) (Fig. S1). For the three pools of *C. crispus* thalli, the yield of the water-extraction procedure was evaluated by weighing the residue R and the supernatant S (after freeze-drying), and comparing this amount to the starting amount of AIR. This allowed evaluating the material loss (L) during the extraction procedure (Table S4). For all pools of *C. crispus* thalli, a higher amount of material was recovered in the supernatant S than in the residue R. The recovery in the supernatant is about 50 % for Gf and Ts and maximum for the Gm pool (~61 %). The yield of the water-extraction procedure was found satisfying, with a maximum percentage of material loss of around 23 % in the case of the Gf pool, and a recovery in the S and R extracts ranging from 77 to 89 % of the initial AIR material.

For all samples, the constitutive polysaccharides of the ECM were hydrolysed up to 30 % (through acid hydrolysis). Fig. 1 shows that, as expected, galactose (Gal) is the dominant detected monosaccharide residue in all fractions, as a tracer of carrageenan polymers. Likewise,

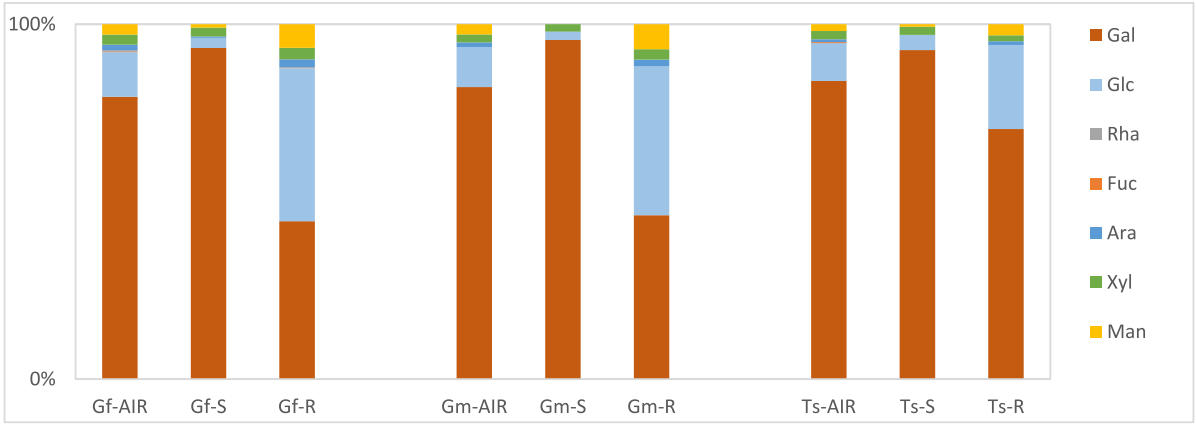

Fig. 1. Relative proportion (% w/(w of total neutral OS without AnGal)) of the different neutral monosaccharides in the AIR, supernatant (S) and residue (R) fractions for the three pools of *C. crispus* individuals. Gal: galactose, Glc: glucose, Rha: rhamnose, Fuc: fucose, Ara: arabinose, Xyl: xylose, Man: mannose.

Gal is more abundant in the S fraction than within the R residues, indicating an enrichment through water extraction as compared to the AIR. It is interesting to note that other glycosides are present in the ECMs of *C. crispus*. Fig. 1 shows that the second important constitutive monosaccharides of ECM are glucose (Glc) residues, which is mainly extracted in the R fraction. Glucose may originate from different polymers in those fractions. In the soluble samples, glucose likely comes from Floridian starch while in the residues it likely comes from cellulose, although a starch origin cannot be excluded. Arabinose (Ara), mannose (Man) and xylose (Xyl) were also detected at trace levels in the extracts. While Man and Ara residues were proportionally enriched in the R fraction, Xyl remained in the same proportion in the S and R fractions compared to the AIR residues. Overall, these results support the hypothesis of other, insoluble, polymers present within the ECM. Crystalline mannans, xylans or glucans have previously been reported in some Gigartinales (Chevenier, Jouanneau, & Ficko-Blean, 2023; Collen et al., 2014; Popper et al., 2011). Even in minor amounts, these polysaccharides may play an important role in the organization and resulting mechanical properties of the ECM. However, it should be noted that one of the major monosaccharides constituting carrageenans, the 3,6-anhydro-D-galactose (AnGal), is not assayed from the method used. It was lost during acid hydrolysis. To complete the results obtained by GC after acid hydrolysis, a determination of the proportion of anhydrogalactoses in soluble fractions (Gf-S, Gm-S and Ts-S) was performed using the colorimetric assay with resorcinol reagent after Yaphe & Arsenault, 1965), since the method can only be applied in solution. The results are shown Fig. S3. The proportion of AnGal was close to 20 % in both Gm and Gf samples which mainly contain κ- and ι-carrageenans. The addition of the two methods therefore enables us to determine the composition of 50 % of both Gm and Gf samples (i.e. 30 % from acidic hydrolysis and 20 % from the AnGal analysis). As expected, the proportion of AnGal was significantly lower (6 %) in the Ts sample that mainly contains λ-carrageenans. Thus, we can define the composition of 41 % of TS samples (i.e. 35 % from acidic hydrolysis and 6 % from the AnGal analysis).

Beyond the phases, natural populations of *C. crispus* can encounter substructure gradients on the shore, such as greater gametophytic bias in low shore populations (Krueger-Hadfield, Collen, Daguin-Thiebaut, & Valero, 2011). To further evaluate possible ECM variations in the three pools in relation to their position on the shore, analyses of two additional *C. crispus* pools of Gf and Ts thalli were made (unfortunately another Gm pool could not be obtained due to fewer confirmed Gm thalli in the field) (high quadrat, Fig. S4). These additional analyses did not reveal a significant difference in term of global ECM composition compared to the low shore quadrat thalli and thus, the low shore quadrat samples were considered as representative of the whole shore in term of ECM composition.

3.3. Structural characterization of carrageenans in the S fraction

The water-soluble ECM components of the Gf, Gm and Ts *C. crispus* thalli were hydrolysed enzymatically to get further insights into the glycan structures. The reaction medium was explored at 0-day (0-D), 1-day (1-D) and after 5 days (5-D) of enzymatic digestion by two structural analytic methods: HPSEC-RI and LC-HR-MS methods.

Three enzymes were used, as stand-alone or in combination: the recombinant *Pseudomonas carrageenovora* κ-carrageenase (GH16), the recombinant *Zobellia galactanivorans* ι-carrageenase (GH82), and the wild type *Pseudomonas carrageenovora* λ-carrageenase (GH150). In this work, we further abbreviate the enzymes as "kappase", "iotase" and "lambdase", respectively. All these enzymes have been previously biochemically, and sometimes structurally, characterized.

The recognition pattern of the active site of the kappase was deduced from gel filtration analysis on pure κ-carrageenans (McLean & Williamson, 1979) and from NMR characterization of pure κ-carrageenans, hybrid κ/ι-carrageenans extracted from *Gigartina skottsbergii*, *Chondracanthus chamissoi*, and *C. crispus* (Guibet et al., 2008), hybrid κ/μ-carrageenans extracted from *Kappaphycus alvarezzi* (Jouanneau et al., 2010) and hybrid κ/β-carrageenans extracted from *Furcellaria* (Correc et al., 2012). The 3D structure of this enzyme has been further determined (Michel et al., 1999). The activity of the iotase was recently validated on ι-carrageenans (Sokolova et al., 2024). Its 3D structure has been characterized but is to date unpublished (Chevenier, Jouanneau, & Ficko-Blean, 2023). Finally, the lambdase was biochemically characterized, and the recognition pattern of the active site was defined on the tetrasporophytic thalli of *Gigartina skottsbergii* (Jouanneau et al., 2010). Its 3D structure is to date undetermined but can confidentially be predicted by Alphafold2. All these enzymes were produced, purified, qualitatively assessed (Fig. S5) and their activities validated on pure commercial substrates (Fig. S6).

3.3.1. HPSEC-RI analyses of the enzymatic hydrolysates

3.3.1.1. Gametophytes. Fig. 2 shows the HPSEC-RI profiles of the gametophytes digested by the kappase and iotase, as stand-alone enzymes or combined. As shown on Fig. 2A, the profiles at different incubation times with the kappase alone are similar (both qualitatively and quantitatively) for female and male thalli. After 1 day of digestion, the profile is comparable to the 0-D profile and suggests the presence of large undigested polymers, with a signal between 40 and 55 min of retention time (RT), and even larger polymers around 36 min of RT. There is almost no signal that can be attributed to smaller oligosaccharides (OS).

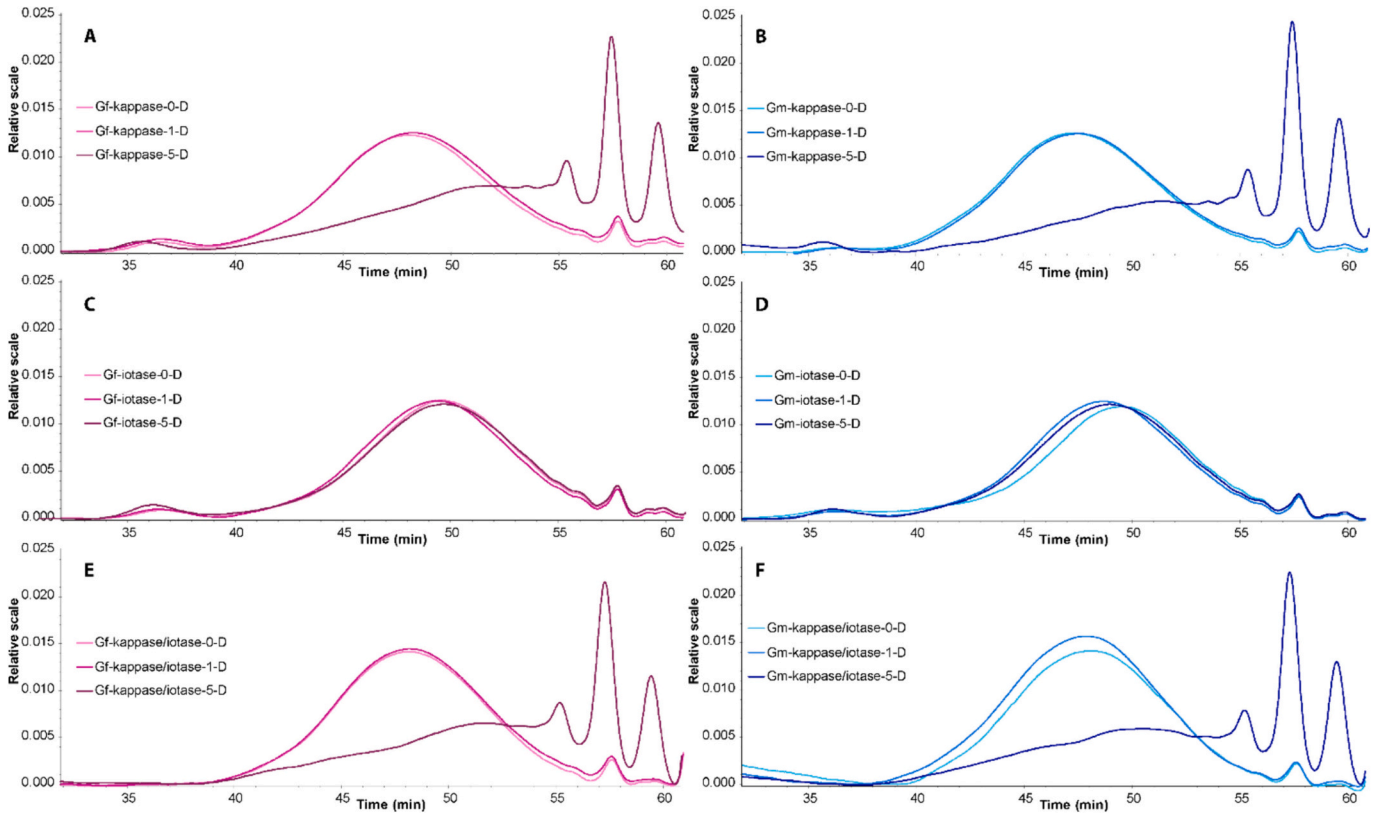

Fig. 2. Enzymatic degradation of *C. crispus* gametophytes (both Gf (panels A, C and E) and Gm (panels B, D and F)) monitored by HPSEC-RI. Profiles for different incubation times are shown with kappase (panels A, B), iotase (panels C, D), and a combination of kappase and iotase (panels E and F).

In contrast, after 5 days, peaks that can be attributed to OS were visualised (RT between 55 and 60 min). This indicates that, as expected, the ECM of the gametophytes contain κ-carrageenans that are efficiently hydrolysed into OS through the action of the kappase after 5 days. However, it is also clear from Fig. 2A that some polymers partially resist the digestion with a kappase, even after 5 days. Fig. 2B displays the profiles of the gametophytes after digestion with the iotase alone. Again, profiles are similar for the female and male gametophytes at all kinetic points. Strikingly, and in contrast to what we observed with the kappase, the signal did not evolve in the course of the kinetics: large polymers did not show a decrease even after 5 days of enzymatic incubation, which suggests that the iotase alone was not able to degrade the polymers in the ECMs of both female and male gametophytes. Finally, Fig. 2C plots the HPSEC-RI profiles obtained on gametophytes using a combination of kappase and iotase enzymes. The profiles resemble those obtained with the kappase alone and do not suggest any synergistic activities of the kappase and iotase on this substrate.

3.3.1.2. Tetrasporophytes. The HPSEC-RI profiles of the tetrasporophytes digested with the lambdase alone or combined with a kappase or iotase are displayed in Fig. 3. The profiles with the lambdase alone or with the two enzymatic cocktails look similar, which suggests that there is no benefit of using a kappase or iotase with the lambdase on the ECM of tetrasporophytes. This result was expected knowing the λ-dominance in tetrasporophytes. If we have a closer look at the profiles with the lambdase (Fig. 3A), peaks that can be attributed to OS (detected at about 52 min of RT) appear early in the course of the digestion (i.e., they are detected in the 0-D sample). This is explained by a very fast action of the lambdase, occurring within the few seconds separating the addition of the enzyme and the boiling procedure. These signals are magnified by a factor 2 after 5 days, and a small peak appears at around 53 min of RT. At all kinetic points, a recalcitrant fraction of larger polymers is observed (peaks ranging from 35 to 55 min of RT), which remains unaltered by an

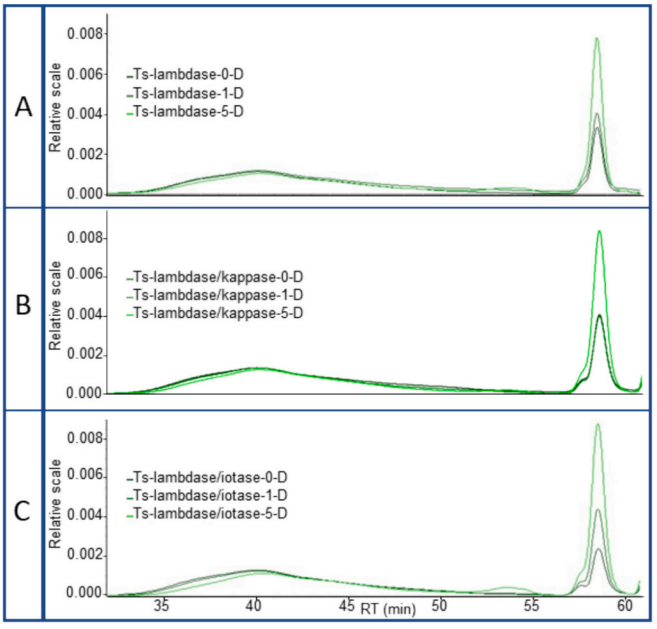

Fig. 3. Enzymatic degradation of *C. crispus* tetrasporophytes monitored by HPSEC-RI. Profiles for different incubation times is shown with the lambdase (panel A), a combination of lambdase and kappase (panel B), and a combination of lambdase and iotase (panel C).

additional use of kappase (Fig. 3B) or iotase (Fig. 3C) with the lambdase. Yet, small differences are observed in the profiles of the 5-D samples after addition of kappase or iotase in the medium: i) the peak at ~53 min of RT slightly decreases with the kappase addition, while this peak

slightly increases when adding the iotase; and ii) the shoulder preceding the major peak (~58 min of RT) slightly increases in intensity in both enzymatic cocktails.

To summarize, the kappase is active on all gametophyte ECM samples after 5 days of incubation, while the iotase seems to be inactive on the gametophyte ECM samples. The lambdase is active on tetrasporophyte ECM samples. The additional use of kappase or iotase does not provide striking differences. Yet, the combination of the lambdase with the iotase on the tetrasporophytes shows additional signals, indicating that the iotase, to some extent, is active on those samples. Average molecular weights for each condition (life stage/enzyme/degradation time) including the controls (undegraded polymers) are indicated in Table S5.

3.3.2. LC-HR-MS analyses of the enzymatic hydrolysates

A combination of ultra-high performance liquid chromatography (UHPLC) and high-resolution mass spectrometry (HR-MS) was used to analyze the same samples As the ones analysed by HPSEC-RI before. The aim of this analysis by HR-MS was to explore in details the oligosaccharide structures released upon enzymatic incubations of the ECM of *C. crispus* gametophytes and tetrasporophytes with the kappase, iotase or lambdase, or binary combinations of those enzymes (Fig. S1). Such detailed structural analyses of the OS products obtained after multiple enzymatic digestions have not been reported to date. Particular care was taken to prevent the erroneous annotation of species that had been desulphated by the analytical method. On all acquisitions, the addition of the ion-pairing agent, which preserves sulfate functions, and the optimization of ionization and transmission conditions demonstrate desulfation of <1 %. As chromatographic separation is based on the number of sulfate functions, these minor species were discarded by aligning retention times.

3.3.2.1. Gametophytes. A large diversity of OS was detected in all enzymatic conditions (i.e., kappase, iotase, and kappase plus iotase) for both female and male gametophytes (between 60 and 80 oligosaccharide species per sample). These OS were categorized into 5 groups and 12 subgroups (Table 1). The first group (6 subgroups), which we named "κ-OS", corresponds to the pure κ-motif and some related motifs; the second group (2 subgroups), named "κ/ι-OS", corresponds to hybrid OS with both κ and ι moieties and some related motifs; the third group (2 subgroups), named "κ/μ-OS", corresponds to hybrid OS with both κ and μ moieties, and some related motifs; the fourth group, named "κ/ι/μ-OS", comprises hybrid OS with κ, ι and μ moieties. OS whose structures do not fit in any of the above groups, form a last group.

A more detailed view of the OS species detected by HR-MS in the Gf thalli under the different enzymatic incubations are presented in Fig. 4. The global quantities of OS released (left panel) are in concordance with those depicted by the HPSEC-RI results, in that only minor amounts of OS are released during incubation with iotase and the addition of iotase to the kappase does not change the profile compared to the use of the kappase alone. This confirms the low activity of the iotase on the ECM of *C. crispus* gametophytes. In the incubation featuring the kappase, a drastic increase (10-fold) in the intensity of the detected OS happens after 5 days compared to the 0-D and 1-D samples, as already observed by the HPSEC-RI analyses (Fig. 2). Regarding the diversity of the OS structures released, the profiles are similar between the 0-D sample and the 1-D sample in both conditions featuring a kappase. A majority of OS bearing κ-motifs (pure κ or hydrated κ, i.e., belonging to subgroups 1 and 2 in Table 1) are detected, as well as a significant proportion of hybrid OS with κ/ι and κ/μ motifs (subgroups 7 and 9). However, after 5 days, this diversity decreases and most of the detected OS belongs to subgroup 1, consisting of pure κ motifs.

No clear difference was observed in any condition between the Gf and Gm thalli. The detailed results for Gm are presented in supplementary information (Fig. S7). However, to highlight a potential heterogeneity relative to the sex of the gametophytes and/or the enzymatic processes, we have monitored the contribution of each subgroup of OS to the peak area of all detected species in both Gm and Gf thalli. In doing so, we focused on the kinetic points at 5-D, and featuring a kappase and the combined use of kappase and iotase (Fig. 5). Pure κ-OS (subgroup 1) predominate, representing about 60 % of the released OS in all conditions. To prevent them from overwhelming the other species, they have been represented on a separate bar graph (left panel). The right-hand panel of Fig. 5, shows the proportions of minor species that are not pure κ-OS. There is no significant variation that can be related to sex. However, contribution of hybrid κ/ι species slightly increases in the OS mixture (15 to 17 % from MS peak areas) with the combined use of the kappase and iotase compared to the kappase alone for both Gf and Gm samples.

3.3.2.2. Tetrasporophytes. As for gametophytes, a diversity of OS was detected in all enzymatic conditions (i.e., lambdase, lambdase and kappase, and lambdase plus iotase) (Fig. 6). This structural diversity is however not as extended as in the gametophytes, with only 4 groups and 8 subgroups that could be constituted (Table 2). The four groups comprise: group 1 (5 subgroups), which we named "λ-OS", corresponds to pure λ motifs and some related motifs; group 2 (no subgroup), named "ι-OS", corresponds to pure ι-motifs; group 3 (no subgroup), named "κ/ι-OS", corresponds to hybrid OS with both κ and ι moieties. OS whose structures do not fit in any of the above groups form group 4.

Focusing on the amount of OS released during the course of incubation (left panel, Fig. 6), there is almost no detectable species in the 0-D samples in all three enzymatic conditions. The lambdase shows a slight activity after one day but only releases a significant number of species in the 5-D sample. Unexpectedly, the combined use of the kappase, or even more the iotase, with the lambdase, increases significantly the amounts

Table 1
Oligosaccharides products identified by UHPLC-HR-MS in the gametophytes samples in all enzymatic digests. Gal: galactose, AnGal: anhydro-galactose, SO_3: sulfate group.

Group	Subgroup	Main motif	Color code	Number of species[(1)]	Comments
κ -OS	1	Pure κ		6	$[1.AnGal+1.Gal+1.SO_3]_n$
	2	Pure κ + H_2O		6	Hydrated κ-OS
	3	Pure κ + 1.Hex + 1.AnGal		3	Potentially hybrib κ/β-OS
	4	Pure κ + 1.Hex		2	Uneven DP - excess of one unsulfated galactose
	5	Pure κ - 1.AnGal		3	Uneven DP - Deficit of one anhydro-galactose
	6	Pure κ + 1.AnGal		3	Uneven DP - excess of one anhydro-galactose
κ/ι -OS	7	Hybrid κ/ι		16	$[1.AnGal+1.Gal+1.SO_3]_x[1.AnGal+1.Gal+2.SO_3]_y$
	8	Hybrid κ/ι - 1.AnGal		7	Uneven DP - Deficit of one anhydro-galactose
κ/μ -OS	9	Hybrid κ/μ		3	$[1.AnGal+1.Gal+1.SO_3]_{n-1}+[2.Gal+2.SO_3]_1$
	10	Hybrid κ/μ + H2O		3	Hydrated Hybrid κ/μ-OS
κ/ι/μ-OS	11	Hybrid κ/ι/μ		2	$[1.AnGal+1.Gal+1.SO_3]_{n-2}+[1.AnGal+1.Gal+2.SO_3]_1 + [2.Gal+2.SO_3]_1$
Others	12	NA		3	OS structures that do not fit in any of the above groups

[(1)]This number is an approximation, it was calculated for the Gf sample incubated for 5 days with the kappase; this number does not account for the diversity of ionic species detected in MS for each OS.

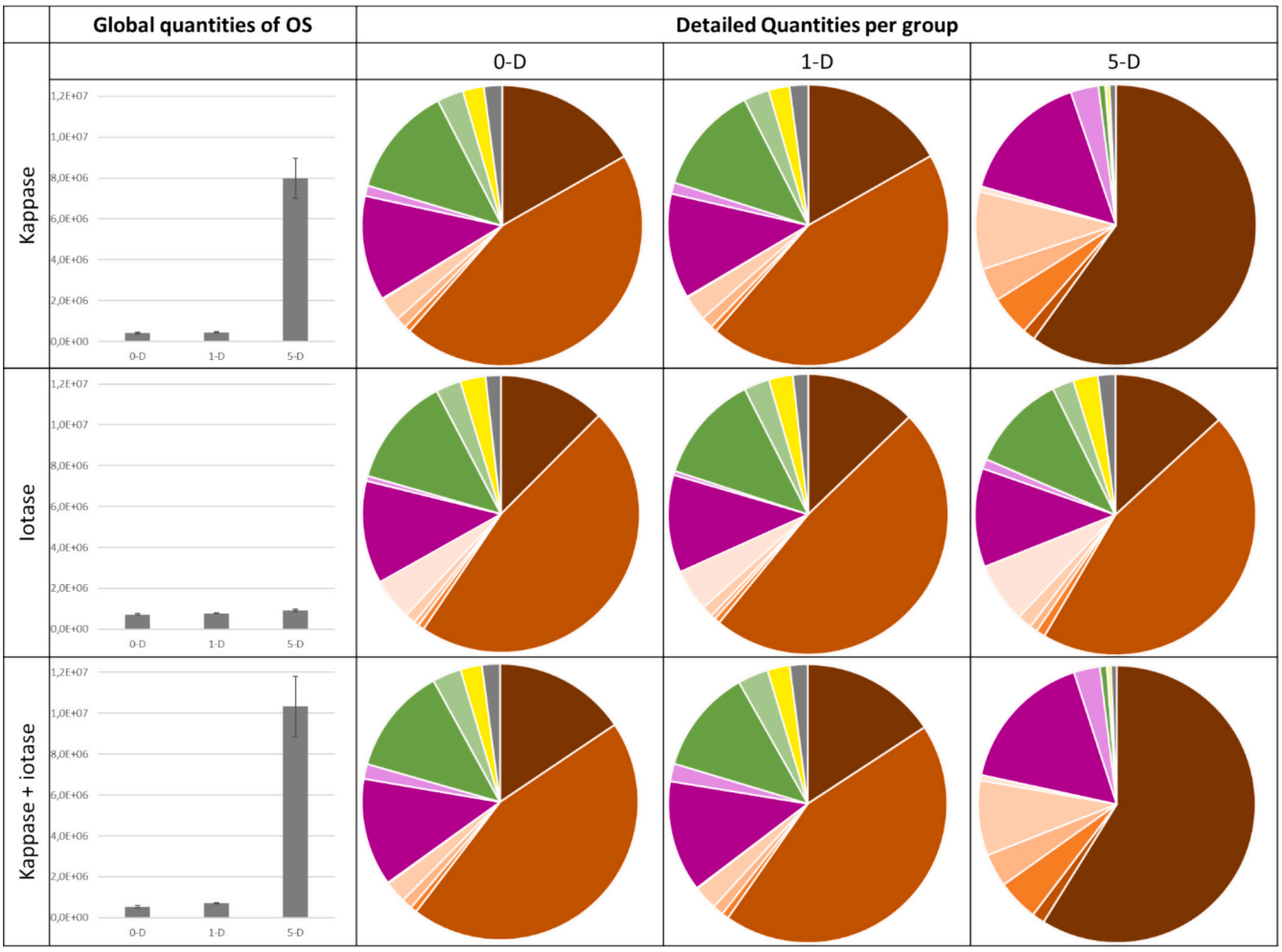

Fig. 4. Quantitative distribution of the different categories of OS released from the female gametophytes. Bar graphs (left side of the figure): MS peak areas were summed for all of the detected OS. Pie charts: contribution of each subgroup. Color code is according to Table 1.

of OS released from the ECM-tetrasporophytes after one day. This singular released is even more prominent after 5 days of digestion. Notably, there is a boost in the OS released when adding the iotase to the lambdase (>2-fold). These results indicate a more contrasted situation between the three enzyme digests than when the samples were analysed through HPSEC-RI. They suggest the presence of minor motifs digested by the iotase, and to a lesser extent by the kappase, in a λ-dominant context.

If we focus on the structural identity of the released OS, the treatment with the lambdase produces—as expected—a rather structurally homogeneous mixture composed of λ-OS and related structures, with pure λ motifs being predominant at 1-D and 5-D. Notably, we observe a significant proportion of under-sulfated species (subgroups 2 to 3 in Table 2) and over-sulfated species (subgroups 4 to 5), which account for 52 % of the annotated structures after 5 days. The addition of the kappase to the lambdase produces a greater diversity with ~15 % of hybrid structures composed of κ and ι moieties. These hybrid κ/ι structures are observed in the same proportion (~13 %) when the iotase is added to the lambdase. However, in this latter medium, a novel category is detected (~5 %) composed of pure ι-OS.

In summary, the LC-HR-MS analyses confirmed the HPSEC-RI results for gametophytes. First, there is no clear difference between females and males. Secondly, the iotase alone does not show an OS-release on the gametophytes while the kappase alone does, mainly after an enzymatic incubation of 5 days. Pure κ-motifs (and related species) were predominant in the degradation of the gametophytes, nevertheless a significant proportion of hybrid structures were also released (κ/ι-, κ/μ- and κ/ι/μ-OS). The addition of the iotase to the kappase slightly enhanced the formation of κ/ι-OS. Such hybrid OS are expected in gametophytes, in which ECM carrageenans are reported to be hybrid polymers made of κ and ι moieties, with the μ moiety being the precursor of the κ moiety.

In the tetrasporophytes, the ECM carrageenans are documented as being essentially constituted of λ-carrageenans. Consistently, the only represented category of OS released after incubation with the lambdase belonged to λ-OS and related compounds. Interestingly however, this category reveals a significant heterogeneity with <50 % of the released OS attributed to pure λ motifs. Under-sulfated species (formed by an additional dimer of hexose accompanied with the loss of one or two sulfate groups) represented 35 % of the OS products after 5 days of incubation with the lambdase, while 17 % of the OS produced were attributed to over-sulfated species (i.e., with one or two extra sulfate groups). Unexpectedly, hybrid motifs of the type κ/ι were also produced when adding the kappase or the iotase to the lambdase, and even pure ι motifs could be detected (~3 %) when combining the iotase to the lambdase. As a general statement, the LC-HR-MS analyses of tetrasporophytes revealed a more contrasted situation between the incubation media (enzymes and time of hydrolysis) than the HPSEC-RI results on the same samples. They also report for the first time the detection of κ/ι motifs in *C. crispus* tetrasporophytes.

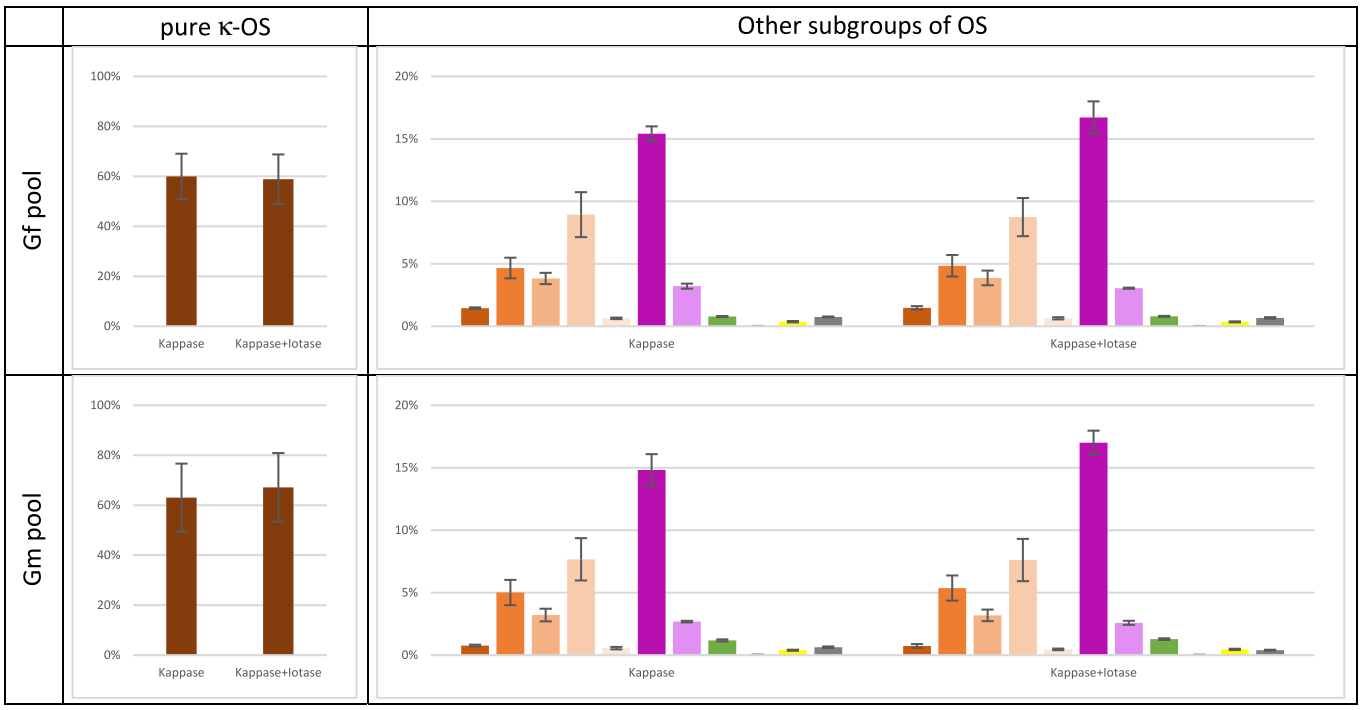

Fig. 5. Contribution of the different subgroups of OS in the mixture for the Gf (top) and Gm (bottom) individual after 5 days of enzymatic incubations with a standalone kappase or with a combination of kappase and iotase. Proportions correspond to MS peak areas normalized by the sum of the peak area of all detected species in the mixture. Left side: contribution of pure κ-OS (subgroup 1 in Table 1). Right side: contribution of other subgroups. Color code is according to Table 1.

4. Discussion and concluding remarks

Although cell wall compositions of carrageenophyte red algae have been previously described and analysed, most studies were done after deconstruction by chemical treatments that often alter the natural occurring structural diversity (Stevenson & Furneaux, 1991). Furthermore, while some attempts have been made to separate life cycle phases—in particular for *C. crispus* (McCandless, Craigie, & Walter, 1973; Stevenson & Furneaux, 1991)—the possibility of cross-contaminations of the algal samples by gametophytes has never been completely ruled out, tempering the conclusions. Besides, the strong viscosity of the λ-carrageenan has always been a drawback for NMR studies, impairing progress on the detailed structural analyses of this polymer.

Here, our investigation combined the microsatellite genotyping to macroscopic analyses in order to sort the thalli, thus excluding any doubt on assigning a specific life cycle phase. Then, we used carrageenan-specific and well-characterized enzymes combined with high-resolution mass spectrometry, to gain a more detailed insight into natural variability in carrageenan contents in the different *C. crispus* phases. As expected, the cell wall composition for male and female gametophytes did not reveal major differences. The first major result of this work is the hybrid nature of the sulfated patterns evidenced in the ECMs of the tetrasporophytes of *C. crispus*. While previous reports essentially describe the sulfated polysaccharide being constituted mainly by pure λ moieties, the picture revealed in our analyses is different. First, a large portion of the oligosaccharides released by the lambdase (>50 % after 5 days) corresponds to under- and over-sulfated species. Besides, the presence of a large resistant fraction that is not hydrolysed by the specific lambdase also witnesses the hybrid nature of this polysaccharide. Even more intriguing, the use of a kappase or iotase in combination with the lambdase revealed a non-negligible quantity of hybrid κ/ι-OS and pure ι-OS carrageenans. In addition to the dominant λ-carrabiose units, a few studies have reported the existence of under-sulfated species in the tetrasporophytes of a variety of Gigartinales (Guibet, 2007; McCandless, West, & Guiry, 1983). One study has also reported the presence of one over-sulfated carrabiose unit in tetrasporophytes of *Gigartina skottsbergii* (Guibet, Kervarec, Genicot, Chevolot, & Helbert, 2006). The same authors were also suggesting the presence of ν, κ and ι moieties in the tetrasporophyte fraction undigested by the lambdase (Guibet, 2007). Overall, our results show that the variety of sulfated polysaccharides in the ECMs of tetrasporophytes of *C. crispus* is much higher and complex than previously described. More generally, up to 50 % of OS deviate from the expected ideal motifs (i.e., from pure κ, pure ι or pure λ) in both gametophytes and tetrasporophytes.

In term of ECM global composition and organization of gametophyte and tetrasporophyte phases of *C. crispus*, as shown for other Gigatinaceae, our analyses showed co-extraction of glycosidic residues other than galactose in the supernatant of the aqueous extracts (Glc but also Man and Xyl). However, the subsequent analyses by LC-HR-MS did not reveal any OS structures demonstrating the presence of polymers other than carrageenans in the ECMs. Several OS structures were detected in which a supernumerary hexose appeared in the typical carrageenan units (odd degrees of polymerization, such as κ + 1.Hex, κ − 1.AnGal, κ + 1.AnGal and hybrid κ/ι − 1.AnGal), although it was not possible to tell whether this supernumerary hexose was Gal, Glc or Man. Of note, most of the additional glycosidic residues (Glc, Man, Xyl and Ara) were found in the water-insoluble residue, which could indicate the occurrence of cellulose or hemicellulosic components such as β-1,3-1,4-glucans or (*gluco*)mannans or a contamination by storage glucans. They seem to be relatively more abundant in the gametophytes rather than in the tetrasporophytes, but a greater biomass of those components would be required to determine their exact nature. Still, our results question how the tetrasporophytes can achieve strong wall-mechanics in the context of λ-motives being dominant. If the amount of carrageenans in the walls can be part of the answer, the different motifs observed (under sulfated and/or over sulfated λ-OS, κ/ι moieties) may also have an impact on the rheology of the wall. The way how these 'novel' motifs are organized within a macromolecular network still need to be assessed. Finally, the number and the nature of the motifs observed from the carrageenan polymers, and more generally from any glycan structure enclaved within a network, will always be dependent on the specificity of the enzyme

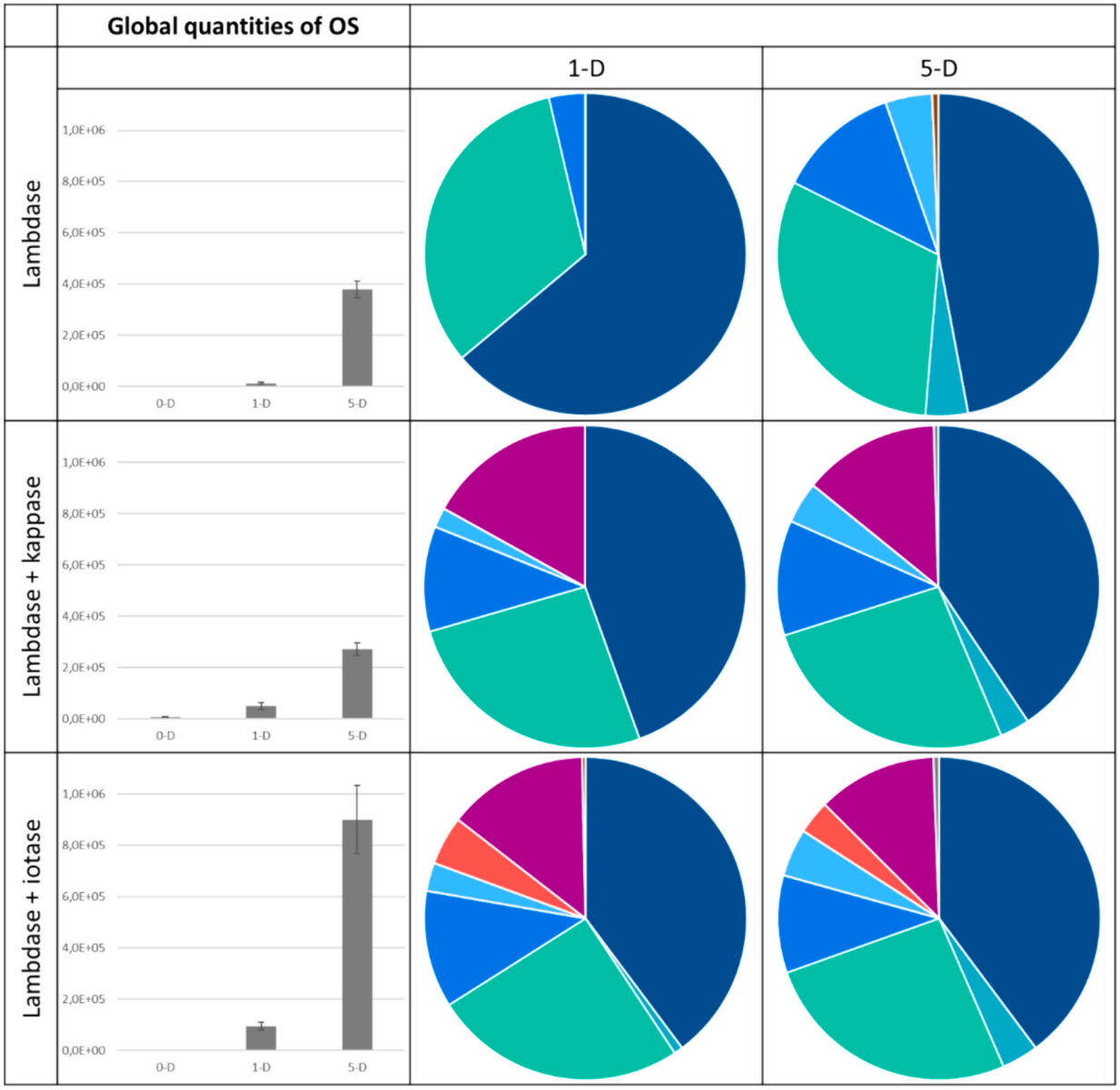

Fig. 6. Quantitative distribution of the different categories of OS released from the tetrasporophyte samples. Bar graphs (left side of the figure): MS peak areas were summed for all of the detected OS. Pie charts: contribution of each subgroup. Color code is according to Table 2.

Table 2
OS products evidenced by UHPLC-HR-MS in the tetrasporophytes samples in all enzymatic conditions. Gal: galactose, AnGal: anhydro-galactose, SO_3: sulfate group.

Group	Subgroup	Main motif	Color code	Number of species[(1)]	Comments
λ-OS	1	Pure λ		3	$[2.Gal+3.SO_3]_n$
	2	Pure λ-2.SO_3		2	under-sulfated species
	3	Pure λ-1.SO_3		3	under-sulfated species
	4	Pure λ+1.SO_3		1	over-sulfated species
	5	Pure λ+2.SO_3		1	over-sulfated species
ι-OS	6	Pure ι		1	$[1.AnGal+1.Gal+1.SO_3]_n$
κ/ ι-OS	7	Hybrid κ/ι		3	$[1.AnGal+1.Gal+1.SO_3]_x[1.AnGal+1.Gal+2.SO_3]_y$
Others	8	NA		1	OS whose structures do not fit any of the above groups

[(1)]This number is an approximation, it was calculated for the Ts sample incubated for 5 days with the lambase + iotase; this number does not account for the diversity of ionic species detected in MS for each OS.

used. The kappase and iotase enzymes have been rarely used in the literature on the Gigartinales tetrasporophytes, due to the assumption that their corresponding substrates were absent from those samples. Our results indicate that such approaches may have led to a partial view of the ECM composition, and that the degrading enzymes should be used more generally prior to a focused investigation.

As an illustration of the aforementioned statement regarding the use of carrageenases and specificity, the occurrence of short OS with hybrid motifs and/or of under- or over-sulfated units indicate that the enzymes can tolerate—to some extent—the presence of carrageenan patterns that differ from the pure κ-, ι- or λ- motifs (Fig. 7). With few exceptions (Guibet et al., 2008; Vilen, Lundqvist, Jouanneau, Helbert, & Sandstrom, 2010), enzymatic activities are generally characterized on pure, ideal, substrates that do not provide information on hybrid patterns that are yet recognized and cleaved by the enzymes, even though with lower efficiency. The hybrid character of the ECMs in all three pools of gametophytes and tetrasporophytes is reflected here in the low efficiency of the enzymes after one day, as compared to their activities on pure substrates. In contrast, the substantial increase in the release of OS after 5 days does highlight that the enzymes can degrade, to some extent, polysaccharides with higher complexity. From the previous enzymatic characterizations and crystal structures of the three carrageenases employed in the present study, we know the number of sub-binding sites that form the active site cleft as described in Guibet et al. (2007), Sokolova et al. (2024) and Michel et al. (2001) and in unpublished results (Chevenier, Jouanneau, & Ficko-Blean, 2023) (Fig. 7). We also know the minimal requirement of ideal motifs that are needed around the cleavage site, as well as the size of the final reaction products (which are DP4 and DP2 for kappase due to the asymmetry of the active suite, which comprises 6 sub-sites (−4 to +2, Fig. 7), and DP4 for iotase and lambdase) as described in Guibet et al. (2007), Sokolova et al. (2024) and Matard-Mann et al. (2017) and in unpublished results (Chevenier, Jouanneau, & Ficko-Blean, 2023). Taken together, this information allows us to deduce that the lambdase is the less tolerant to hybrid patterns, but tolerates modifications such as under- or over-sulfations; at least for the six central sub-binding sites that need to be covered by the substrate for the cleavage to occur (leading to DP4 as major and DP2 as minor final products). Indeed, the absence of 3,6-anhydro-bridge and the sulfation at position O6, which is protruding from the saccharide-unit in λ-carrageenan, are more drastic modifications than the absence or addition of a sulfate group on position O2 between κ- and ι-carrageenan. Moreover, the kappase and the iotase specifically require the O4-sulfate group in galactose at the crucial position −1 at the cleavage site, while this position is systematically un-sulfated in λ-carrageenan. Nevertheless, we might also consider another explanation in that the λ-polysaccharide chains potentially only contain under- or over-sulfations, but are not hybrid with κ- and ι- (and precursor) motifs, forming two separated while intertangled polysaccharide chains.

Another major result concerns the presence of κ/ι-hybrid polysaccharides, which differs between tetrasporophytes and gametophytes. The kappase releases, among others, pure κ-OS in the gametophytes while in the tetrasporophytes, such structures do not occur. Conversely, no OS was released with the iotase in the gametophytes while hybrid κ/ι-OS and pure ι-OS were evidenced in the tetrasporophytes. Given what we know about the mode of action of the iotase (with eight subsites), we can postulate that the distribution of ι motifs on hybrid κ/ι-carrageenan chains in gametophytes is not adapted for an optimal activity of this iotase. Indeed, the enzyme specifically recognizes ι-motifs

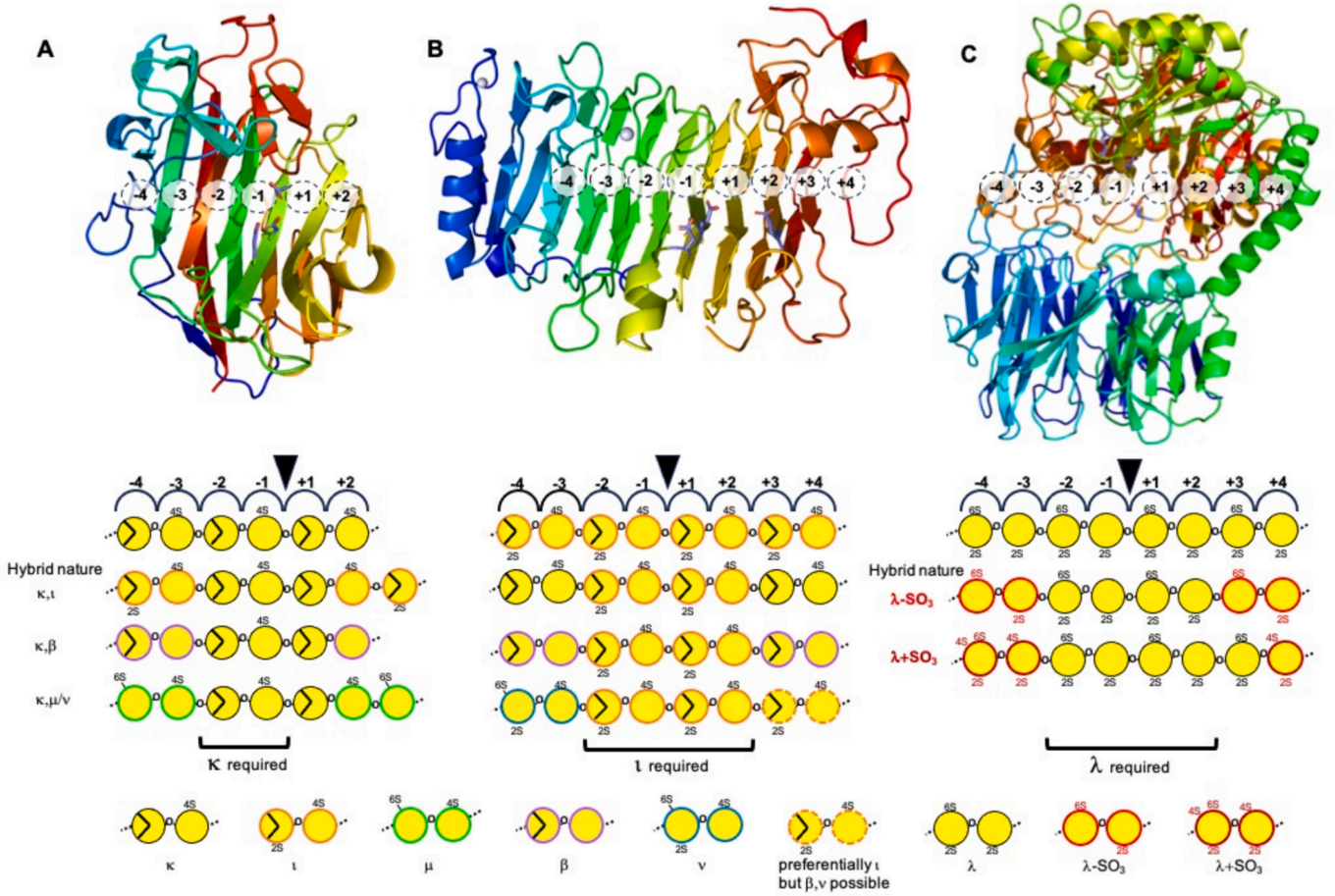

Fig. 7. Ribbon and schematic representations of the active site clefts of kappase (A), iotase (B) and lambdase (C). The subsite nomenclature (Davies, Wilson, & Henrissat, 1997) defines site −4 at the non-reducing end to +4 at the reducing end with the cleavage occurring between −1 and +1 (black arrowhead in the schematic representations). In all three carrageenases, the central positions, especially sites −1 and −2 (also +1 and +2 for iotase and lambdase), are restricted to the carrageenan motif related to the substrate specificity of the enzyme. The color code of the diverse carrageenan motifs that are tolerated at different sub-sites are given at the bottom of the figure.

for the four central sub-binding sites (Fig. 7B), and κ-motifs or other modifications are only tolerated at sub-sites −3, −4 and +3 and +4. We cannot exclude the possibility that the organization or accessibility of ι-motifs in the ECM of gametophytes is not adapted to the conditions for an optimal activity of the Zg-iotase. Hybrid κ/ι-polysaccharides would be a sequence of κ-subunits with only few ι-moieties occasionally interspersed, with the absence of DP6 ι-stretches. In tetrasporophytes, on the other hand, the iotase was able to access its substrates, which suggests a different distribution of ι-motifs in the hybrid κ/ι-polysaccharide chains and/or a different organization of the ECM compared to gametophytes. In this case, the polysaccharide appears to be a chain of ι-subunits (with at least blocks of DP6) with fewer κ-moieties occasionally interspersed. Another possibility we can't rule out with these observed differences would be a different proportion or distribution of κ- or ι-carrageenan precursors (motifs μ and ν).

The present analyses of the ECMs of *C. crispus*, in light with the recent availability of genomic and transcriptomic resources, allow further speculation on the biosynthetic pathways of its constitutive carrabiose units. While a putative biosynthetic pathway for carrageenans has been generally accepted and largely used (Chevenier, Jouanneau, & Ficko-Blean, 2023; Craigie & Wong, 1979; Ficko-Blean, Hervé, & Michel, 2015), it becomes clear from our results that some units—and the corresponding synthesis steps to build them—are missing on the way. The over-sulfated blocks, such as those found in the *C. crispus* tetrasporophytes, have never been incorporated into this biosynthetic scheme, yet they are quantitatively significant and cannot be ignored. Given the rare occurrence of carrabiose units featuring a 3,6-anhydro-bridge in tetrasporophytes as compared to gametophytes, fewer sulfurylase genes should be needed. Yet, the reverse has been observed in transcriptomic data (Lipinska, Collen, Krueger-Hadfield, Mora, & Ficko-Blean, 2020), suggesting a greater diversity in enzymatic activities as previously thought, and by extension, a greater structural diversity as presently claimed. Among the 7 carbohydrate-sulfotransferases encoded by the *C. crispus* genome, 5 were differentially expressed among the phases and 4 were specifically over-expressed in the tetrasporophytes. They could potentially be involved in the synthesis of the over-sulfated motifs found along the λ-carrageenans. Galactosyl-sulfurylases are a rare case of a multigenic family in *C. crispus*. Among the 16 genes identified, only 2 involved in the conversion of ν- to ι-carrageenan have been biochemically validated (i.e., CHC_T00008501001 known as sulfurylase I and CHC_T00009416001 known as sulfurylase II) (Genicot-Joncour et al., 2009). The conversion of μ- to κ-carrageenan has also been demonstrated, most interestingly in both phases (Wong & Craigie, 1978). The corresponding gene(s) are unknown, yet they must be within the 14 genes left. Interestingly, the gene of sulfurylase II is significantly over-expressed in the tetrasporophytes and would represent a strong candidate for the synthesis of ι-motifs. However, ν-carrabiose precursors have not been detected in our dataset. Either they are of minor occurrence and immediately converted, or sulfurylase II might also accommodate additional motifs among those newly identified in the present study, in addition to the ν-motifs found in the sole ν/ι-carrageenans tested (Genicot-Joncour et al., 2009). Only one gene closely related to sulfurylase II was significantly upregulated in gametophytes relative to tetrasporophytes. It is thus tempting to speculate its implication in the synthesis of either κ- or ι-carrageenans in the gametophytes, through the conversion of μ- and ν-motifs, respectively. This leaves another 9 genes (in addition to sulfurylase II) upregulated in tetrasporophytes relative to gametophytes. They would be good candidates for the conversion of some λ- to θ-carrabiose units (i.e., under-sulfated), but could also hypothetically be involved in the desulfation of the over-sulfated motifs that were found outside the λ-motifs. This would however imply that these sulfurylases feature a sulfatase-like activity, without shaping 3,6-anhydro-bridges, since this feature was not found in our dataset outside the κ/ι-motifs. In the context of the total absence of canonical sulfatases in the genome of *C. crispus*, this hypothesis could become plausible (Chevenier, Jouanneau, & Ficko-Blean, 2023).

Our data indicate that ECM composition and architecture, and more specifically the structure of the carrageenan chains in *C. crispus*, are of greater diversity as previously thought. The new analytical tools that we employed in the current study, together with genomic resources, would be relevant as well for a deeper investigation of ECM dynamics in *C. crispus* during the infection by its green algal pathogen *Ulvella* (*Acrochaete*) *operculata*. Indeed, some past research on this pathosystem have elegantly demonstrated a drastically different resistance response within gametophytes and tetrasporophytes. It was also demonstrated that the interaction was mediated by carrageenan-motifs (Bouarab, Potin, Correa, & Kloareg, 1999). Yet, the molecular basis of these differential interactions has never been explored, nor the changes upon infection in the carrageenan composition of the two phases. Together, these data will inform our understanding of complex life cycles with alternations between isomorphic phases.

Fundings and acknowledgements

This work received financial support (salary AL) from the Région Pays-de-la-Loire, the Région Bretagne (through the GlycoOuest project) and from the Cargill Company. The collection of *Chondrus crispus* was supported by a PhD fellowship funded by CNRS and Région Bretagne (ARED 211-B2-9: PIOKA) to SAKH as well funding from GIS-Europôle Mer (2010) and ASSEMBLE EU FP7 research infrastructure initiative to MV. The funding body was involved in the approval of the initial design of the study. We would like to thank Gino Mangiante and Patrick Boulenguer (from the Cargill Company) for their helpful discussions throughout the project.

CRediT authorship contribution statement

David Ropartz: Writing – review & editing, Writing – original draft, Validation, Supervision, Project administration, Investigation, Funding acquisition, Data curation, Conceptualization. **Adrien Lissarrague:** Writing – review & editing, Methodology, Investigation, Formal analysis, Data curation. **Murielle Jam:** Writing – review & editing, Validation, Investigation, Formal analysis, Data curation. **Diane Jouanneau:** Writing – review & editing, Validation, Investigation, Formal analysis, Data curation. **Sophie Le Gall:** Writing – review & editing, Validation, Formal analysis, Data curation. **Bastien Annic:** Writing – review & editing, Formal analysis, Data curation. **Mathieu Fanuel:** Writing – review & editing, Formal analysis, Data curation. **Stacy A. Krueger-Hadfield:** Writing – review & editing, Formal analysis, Data curation. **Myriam Valéro:** Writing – review & editing, Formal analysis, Data curation. **Mirjam Czjzek:** Writing – review & editing, Writing – original draft, Project administration, Funding acquisition, Conceptualization. **Hélène Rogniaux:** Writing – review & editing, Writing – original draft, Supervision, Project administration, Funding acquisition, Conceptualization. **Cécile Hervé:** Writing – review & editing, Writing – original draft, Supervision, Project administration, Funding acquisition, Conceptualization.

Declaration of competing interest

The authors declare that they have no known competing financial interests or personal relationships that could have appeared to influence the work reported in this paper.

Data availability

Data will be made available on request.

Appendix A. Supplementary data

Supplementary data to this article can be found online at https://doi.org/10.1016/j.carbpol.2024.122737.

References

Ahmadi, A., Moghadamtousi, S. Z., Abubakar, S., & Zandi, K. (2015). Antiviral potential of algae polysaccharides isolated from marine sources: A review. *BioMed Research International, 2015*, Article 825203. https://doi.org/10.1155/2015/825203

Anastyuk, S. D., Barabanova, A. O., Correc, G., Nazarenko, E. L., Davydova, V. N., Helbert, W., … Yermak, I. M. (2011). Analysis of structural heterogeneity of κ/β-carrageenan oligosaccharides from *Tichocarpus crinitus* by negative-ion ESI and tandem MALDI mass spectrometry. *Carbohydrate Polymers, 86*(2), 546–554. https://doi.org/10.1016/j.carbpol.2011.04.081

Bouarab, K., Potin, P., Correa, J., & Kloareg, B. (1999). Sulfated oligosaccharides mediate the interaction between a marine red alga and its green algal pathogenic endophyte. *Plant Cell, 11*(9), 1635–1650. https://doi.org/10.1105/tpc.11.9.1635

Carrington, E., Grace, S. P., & Chopin, T. (2001). Life history phases and the biomechanical properties of the red alga *Chondrus crispus* (Rhodophyta). *Journal of Phycology, 37*(5), 699–704. https://doi.org/10.1046/j.1529-8817.2001.00169.x

Cheong, K.-L., Qiu, H.-M., Du, H., Liu, Y., & Khan, B. M. (2018). Oligosaccharides derived from red seaweed: Production, properties, and potential health and cosmetic applications. *Molecules, 23*(10), 2451. https://doi.org/10.3390/molecules23102451

Chevenier, A., Jouanneau, D., & Ficko-Blean, E. (2023). Carrageenan biosynthesis in red algae: A review. *The Cell Surface, 9*, Article 100097. https://doi.org/10.1016/j.tcsw.2023.100097

Collen, J., Cornish, M. L., Craigie, J., Ficko-Blean, E., Herve, C., Krueger-Hadfield, S. A., Leblanc, C., Michel, G., Potin, P., Tonon, T., & Boyen, C. (2014). *Chondrus crispus*—A present and historical model organism for red seaweeds. In N. Bourgougnon (Éd.), Sea plants (Vol. 71, p. 53–89). Academic Press Ltd.-Elsevier Science Ltd. doi: https://doi.org/10.1016/B978-0-12-408062-1.00003-2.

Collen, J., Porcel, B., Carre, W., Ball, S. G., Chaparro, C., Tonon, T., … Boyen, C. (2013). Genome structure and metabolic features in the red seaweed *Chondrus crispus* shed light on evolution of the Archaeplastida. *Proceedings of the National Academy of Sciences of the United States of America, 110*(13), 5247–5252. https://doi.org/10.1073/pnas.1221259110

Collen, P. N., Lemoine, M., Daniellou, R., Guegan, J.-P., Paoletti, S., & Helbert, W. (2009). Enzymatic degradation of κ-carrageenan in aqueous solution. *Biomacromolecules, 10*(7), 1757–1767. https://doi.org/10.1021/bm9001766

Correc, G., Barabanova, A., Tuvikene, R., Truus, K., Yermak, I., & Helbert, W. (2012). Comparison of the structures of hybrid κ-/β-carrageenans extracted from *Furcellaria lumbricalis* and *Tichocarpus crinitus*. *Carbohydrate Polymers, 88*(1), 31–36. https://doi.org/10.1016/j.carbpol.2011.11.052

Craigie, J., & Wong, K. (1979). Carrageenan biosynthesis. *Proceedings of International Seaweed Symposium, 9*, 595–609.

Davies, G. J., Wilson, K. S., & Henrissat, B. (1997). Nomenclature for sugar-binding subsites in glycosyl hydrolases. *Biochemical Journal, 321*, 557–559. https://doi.org/10.1042/bj3210557

Dong, Y., Wei, Z., & Xue, C. (2021). Recent advances in carrageenan-based delivery systems for bioactive ingredients: A review. *Trends in Food Science & Technology, 112*, 348–361. https://doi.org/10.1016/j.tifs.2021.04.012

Ficko-Blean, E., Hervé, C., & Michel, G. (2015). Sweet and sour sugars from the sea: The biosynthesis and remodeling of sulfated cell wall polysaccharides from marine macroalgae. *Perspectives in Phycology*, 51–64. https://doi.org/10.1127/pip/2015/0028

García Tasende, M., Cid, M., & Fraga, M. I. (2012). Spatial and temporal variations of *Chondrus crispus* (Gigartinaceae, Rhodophyta) carrageenan content in natural populations from Galicia (NW Spain). *Journal of Applied Phycology, 24*, 941–951. https://doi.org/10.1007/s10811-011-9715-y

Genicot-Joncour, S., Poinas, A., Richard, O., Potin, P., Rudolph, B., Kloareg, B., & Helbert, W. (2009). The cyclization of the 3,6-anhydro-galactose ring of ι-carrageenan is catalyzed by two D-galactose-2,6-sulfurylases in the red alga *Chondrus crispus*. *Plant Physiology, 151*(3), 1609–1616. https://doi.org/10.1104/pp.109.144329

Giles, K., Ujma, J., Wildgoose, J., Pringle, S., Richardson, K., Langridge, D., & Green, M. (2019). A cyclic ion mobility-mass spectrometry system. *Analytical Chemistry, 91*(13), 8564–8573. https://doi.org/10.1021/acs.analchem.9b01838

Guibet, M. (2007). Analyse structurale des carraghénanes par hydrolyse enzymatique. http://www.theses.fr/2007BRES2003/document.

Guibet, M., Boulenguer, P., Mazoyer, J., Kervarec, N., Antonopoulos, A., Lafosse, M., & Helbert, W. (2008). Composition and distribution of carrabiose moieties in hybrid κ-/ι-carrageenans using carrageenases. *Biomacromolecules, 9*(1), 408–415. https://doi.org/10.1021/bm701109r

Guibet, M., Colin, S., Barbeyron, T., Genicot, S., Kloareg, B., Michel, G., & Helbert, W. (2007). Degradation of λ-carrageenan by *Pseudoalteromonas carrageenovora* λ-carrageenase: A new family of glycoside hydrolases unrelated to κ- and ι-carrageenases. *Biochemical Journal, 404*, 105–114. https://doi.org/10.1042//BJ20061359

Guibet, M., Kervarec, N., Genicot, S., Chevolot, Y., & Helbert, W. (2006). Complete assignment of ^{1}H and ^{13}C NMR spectra of *Gigartina skottsbergii* λ-carrageenan using carrabiose oligosaccharides prepared by enzymatic hydrolysis. *Carbohydrate Research, 341*(11), 1859–1869. https://doi.org/10.1016/j.carres.2006.04.018

Jouanneau, D., Boulenguer, P., Mazoyer, J., & Helbert, W. (2010). Complete assignment of ^{1}H and ^{13}C NMR spectra of standard neo-ι-carrabiose oligosaccharides. *Carbohydrate Research, 345*(4), 547–551. https://doi.org/10.1016/j.carres.2009.12.004

Jouanneau, D., Guibet, M., Boulenguer, P., Mazoyer, J., Smietana, M., & Helbert, W. (2010). New insights into the structure of hybrid κ-/μ-carrageenan and its alkaline conversion. *Food Hydrocolloids, 24*(4), 452–461. https://doi.org/10.1016/j.foodhyd.2009.11.012

Kloareg, B., Badis, Y., Cock, J. M., & Michel, G. (2021). Role and evolution of the extracellular matrix in the acquisition of complex multicellularity in eukaryotes: A macroalgal perspective. *Genes, 12*(7), 1059. https://doi.org/10.3390/genes12071059

Krueger-Hadfield, S. A., Collen, J., Daguin-Thiebaut, C., & Valero, M. (2011). Genetic population structure and mating system in *Chondrus crispus* (Rhodophyta). *Journal of Phycology, 47*(3), 440–450. https://doi.org/10.1111/j.1529-8817.2011.00995.x

Krueger-Hadfield, S. A., Roze, D., Correa, J. A., Destombe, C., & Valero, M. (2015). O father where art thou? Paternity analyses in a natural population of the haploid-diploid seaweed *Chondrus crispus*. *Heredity, 114*(2), 185–194. https://doi.org/10.1038/hdy.2014.82

Krueger-Hadfield, S. A., Roze, D., Mauger, S., & Valero, M. (2013). Intergametophytic selfing and microgeographic genetic structure shape populations of the intertidal red seaweed *Chondrus crispus*. *Molecular Ecology, 22*(12), 3242–3260. https://doi.org/10.1111/mec.12191

Lazo, M., Greenwell, M., & Mclachlan, J. (1989). Population-structure of *Chondrus-Crispus* stackhouse (Gigartinaceae, Rhodophyta) along the coast of Prince Edward Island, Canada—Distribution of gametophytic and sporophytic fronds. *Journal of Experimental Marine Biology and Ecology, 126*(1), 45–58.

Lipinska, A. P., Collen, J., Krueger-Hadfield, S. A., Mora, T., & Ficko-Blean, E. (2020). To gel or not to gel: Differential expression of carrageenan-related genes between the gametophyte and tetrasporophyte life cycle stages of the red alga *Chondrus crispus*. *Scientific Reports, 10*(1), 11498. https://doi.org/10.1038/s41598-020-67728-6

Matard-Mann, M., Bernard, T., Leroux, C., Barbeyron, T., Larocque, R., Prechoux, A., … Czjzek, M. (2017). Structural insights into marine carbohydrate degradation by family GH16-carrageenases. *Journal of Biological Chemistry, 292*(48), 19919–19934. https://doi.org/10.1074/jbc.M117.808279

McCandless, E., Craigie, J., & Walter, J. (1973). Carrageenans in gametophytic and sporophytic stages of *Chondrus-Crispus*. *Planta, 112*(3), 201–212. https://doi.org/10.1007/BF00385324

McCandless, E., West, J., & Guiry, M. (1983). Carrageenan patterns in the Gigartinaceae. *Biochemical Systematics and Ecology, 11*(3), 175–182. https://doi.org/10.1016/0305-1978(83)90049-2

McLean, M. W., & Williamson, F. B. (1979). χ-Carrageenase from *Pseudomonas carrageenovora*. *European Journal of Biochemistry, 93*(3), 553–558. https://doi.org/10.1111/j.1432-1033.1979.tb12854.x

Michel, G., Barbeyron, T., Flament, D., Vernet, T., Kloareg, B., & Dideberg, O. (1999). Expression, purification, crystallization and preliminary X-ray analysis of the κ-carrageenase from *Pseudoalteromonas carrageenovora*. *Acta Crystallographica Section D—Biological Crystallography, 55*, 918–920. https://doi.org/10.1107/S0907444998018526

Michel, G., Chantalat, L., Duee, E., Barbeyron, T., Henrissat, B., Kloareg, B., & Dideberg, O. (2001). The κ-carrageenase of *P-carrageenovora* features a tunnel-shaped active site: A novel insight in the evolution of clan-B glycoside hydrolases. *Structure, 9*(6), 513–525. https://doi.org/10.1016/S0969-2126(01)00612-8

Pacheco-Quito, E.-M., Ruiz-Caro, R., & Veiga, M.-D. (2020). Carrageenan: Drug delivery systems and other biomedical applications. *Marine Drugs, 18*(11), 583. https://doi.org/10.3390/md18110583

Peaucelle, A., Braybrook, S., & Hoefte, H. (2012). Cell wall mechanics and growth control in plants: The role of pectins revisited. *Frontiers in Plant Science, 3*, 121. https://doi.org/10.3389/fpls.2012.00121

Pluskal, T., Castillo, S., Villar-Briones, A., & Oresic, M. (2010). MZmine 2: Modular framework for processing, visualizing, and analyzing mass spectrometry-based molecular profile data. BMC Bioinformatics, 11, 395. doi:https://doi.org/10.1186/1471-2105-11-395.

Popper, Z. A., Michel, G., Hervé, C., Domozych, D. S., Willats, W. G. T., Tuohy, M. G., … Stengel, D. B. (2011). Evolution and diversity of plant cell walls: From algae to flowering plants. *Annual Review of Plant Biology, 62*(1), 567–590. https://doi.org/10.1146/annurev-arplant-042110-103809

Prechoux, A., & Helbert, W. (2014). Preparation and detailed NMR analyses of a series of oligo-α-carrageenans. *Carbohydrate Polymers, 101*, 864–870. https://doi.org/10.1016/j.carbpol.2013.10.007

Rupert, R., Rodrigues, K. F., Thien, V. Y., & Yong, W. T. L. (2022). Carrageenan from *Kappaphycus alvarezii* (Rhodophyta, Solieriaceae): Metabolism, structure, production, and application. *Frontiers in Plant Science, 13*, Article 859635. https://doi.org/10.3389/fpls.2022.859635

Sokolova, E., Jouanneau, D., Chevenier, A., Jam, M., Desban, N., Colas, P., … Michel, G. (2024). Enzymatically-derived oligo-carrageenans interact with α-Gal antibodies and Galectin-3. *Carbohydrate Polymers, 324*, Article 121563. https://doi.org/10.1016/j.carbpol.2023.121563

Stevenson, T. T., & Furneaux, R. H. (1991). Chemical methods for the analysis of sulphated galactans from red algae. *Carbohydrate Research, 210*, 277–298. https://doi.org/10.1016/0008-6215(91)80129-B

Vilen, E. M., Lundqvist, L. C. E., Jouanneau, D., Helbert, W., & Sandstrom, C. (2010). NMR study on hydroxy protons of κ- and κ/μ-hybrid carrageenan oligosaccharides: Experimental evidence of hydrogen bonding and chemical exchange interactions in κ/μ oligosaccharides. *Biomacromolecules, 11*(12), 3487–3494. https://doi.org/10.1021/bm100994x

Wong, K., & Craigie, J. (1978). Sulfohydrolase activity and carrageenan biosynthesis in *Chondrus-Crispus* (rhodophyceae). *Plant Physiology, 61*(4), 663–666. https://doi.org/10.1104/pp.61.4.663

Yaphe, W., & Arsenault, G. (1965). Improved resorcinol reagent for determination of fructose and of 3,6-anhydrogalactose in polysaccharides. *Analytical Biochemistry, 13*(1), 143. https://doi.org/10.1016/0003-2697(65)90128-4

Yermak, I., Anastyuk, S., Kravchenko, A., Helbert, W., Glazunov, V., Shulgin, A., … Prassolov, V. (2021). New insights into the structure of kappa/beta-carrageenan: A

novel potential inhibitor of HIV-1. *International Journal of Molecular Sciences, 22*(23), 12905. https://doi.org/10.3390/ijms222312905

Zablackis, E., & Perez, J. (1990). A partially pyruvated carrageenan from Hawaiian *Grateloupia-Filicina* (cryptonemiales, Rhodophyta). *Botanica Marina, 33*(3), 273–276. https://doi.org/10.1515/botm.1990.33.3.273

Zia, K. M., Tabasum, S., Nasif, M., Sultan, N., Aslam, N., Noreen, A., & Zuber, M. (2017). A review on synthesis, properties and applications of natural polymer based carrageenan blends and composites. *International Journal of Biological Macromolecules, 96*, 282–301. https://doi.org/10.1016/j.ijbiomac.2016.11.095